Dual Polymerization Pathway for Polyolefin-Polar Block Copolymer Synthesis via MILRad: Mechanism and Scope

Huong Dau, Anthony Keyes, Hatice E. Basbug Alhan, Estela Ordonez, Enkhjargal Tsogtgerel, Anthony P. Gies, Evelyn Auyeung, Zhe Zhou, Asim Maity, Anuvab Das, David C. Powers, Dain B. Beezer,* and Eva Harth*

Cite This: https://dx.doi.org/10.1021/jacs.0c10588

Read Online

ACCESS | Metrics & More | Article Recommendations | SI Supporting Information

ABSTRACT: This work explores the mechanism whereby a cationic diimine Pd(II) complex combines coordination insertion and radical polymerization to form polyolefin—polar block copolymers. The initial requirement involves the insertion of a single acrylate monomer into the Pd(II)—polyolefin intermediates, which generate a stable polymeric chelate through a chain-walking mechanism. This thermodynamically stable chelate was also found to be photochemically inactive, and a unique mechanism was discovered which allows for radical polymerization. Rate-determining opening of the chelate by an ancillary ligand followed by additional chain walking allows the metal to migrate to the α-carbon of the acrylate moiety. Ultimately, the molecular

parameters necessary for blue-light-triggered Pd—C bond homolysis from this α-carbon to form a carbon-centered macroradical species were established. This intermediate is understood to initiate free radical polymerization of acrylic monomers, thereby facilitating block copolymer synthesis from a single Pd(II) complex. Key intermediates were isolated and comprehensively characterized through exhaustive analytical methods which detail the mechanism while confirming the structural integrity of the polyolefin—polar blocks. Chain walking combined with blue-light irradiation functions as the mechanistic switch from coordination insertion to radical polymerization. On the basis of these discoveries, robust di- and triblock copolymer syntheses have been demonstrated with olefins (ethylene and 1-hexene) which produce amorphous or crystalline blocks and acrylics (methyl acrylate, ethyl acrylate, n-butyl acrylate, and methyl methacrylate) in broad molecular weight ranges and compositions, yielding AB diblocks and BAB triblocks.
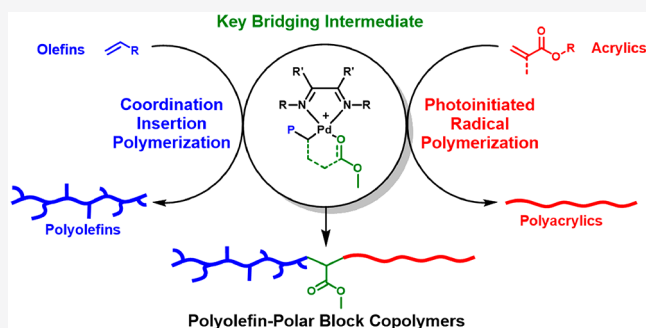
INTRODUCTION

Polyolefin—polar block copolymers are of interest due to their unique physical properties which arise from the covalent linkage of two or more distinct monomers in a block-type architecture. The combination of polar and nonpolar properties in a block copolymer can greatly tune important properties such as toughness, adhesion, surface properties, solvent resistance, etc.[1] Specifically, the phase separation of block copolymers allows for properties that arise from their microstructure, whose application will boost the performance of already known plastics and offer avenues to unexplored applications.[2] However, the limited platforms available to generate these highly valued materials has led to a scarcity of polyolefin—polar block copolymers and serve as the bottleneck for future plastic development.[3] In part, this can be attributed to the fundamental difference in reactivity between polar and nonpolar monomers and has led to divergent synthetic techniques optimized for each monomer class. These approaches can now accommodate a few specific polar and nonpolar monomers by tuning the tolerance and reactivity of

an established platform.[2e,4] However, an alternative way of thinking abandons improving the tolerance of a single polymerization technique and instead seeks to develop a methodology which merges multiple polymerization platforms using a single metal complex, accommodating polar and nonpolar monomers.[5]

An attractive approach that would be of broad interest is the linking of coordination insertion and radical polymerization techniques, which have been used separately to polymerize nonpolar and polar monomers with great control, respectively. An ideal candidate to achieve this duality is Brookhart's palladium(II) diimine complex, which has been well studied in terms of coordination insertion polymerization,[6] while also

having been reported to initiate radical polymerization.[7] However, attempts to bring these two polymerization techniques together have mostly been unsuccessful and highlight the mechanistic obstacles associated with this approach.[7a−c] In an attempt to copolymerize olefins and acrylics with Brookhart catalysts, Espinet et al. sought to access a dual-polymerization platform in which congruent coordination insertion and radical polymerization would generate copolymers.[7b] In a similar approach, Ye et al. observed that a mixture of homopolymers is obtained as a result of the decoupled coordination insertion and radical mechanisms.[7f] Monteil et al. have shown that a salicylaldiminato Ni(II) catalyst performs both coordination insertion and radical polymerization, yet the radical polymerization is only possible following the irreversible reductive elimination of the Ni(II) species to Ni(0).[8] As such, radical polymerization is only attainable from the deactivated catalysts which no longer contain the polyolefin, preventing block copolymer formation. Recently, a method to successfully combine coordination insertion with radical polymerization, metal−organic insertion light-initiated radical (MILRad) polymerization, has been developed in our group, producing for the first time polyolefin−polar block copolymers with a single Pd(II) complex.[7d] However, this approach was limited to low-molecular-weight olefin block segments, and the integrity of the blocks remained a contentious facet of the work, as no mechanistic understanding could explain the success of this method.

We believe an understanding of the mechanism by which the Brookhart-type complex can generate radicals will provide the necessary insight needed for the generation of macroradical initiators which are capable of block copolymer synthesis. Herein, we report a comprehensive mechanism for block copolymer formation based upon the isolation and characterization of key intermediates, combined with a detailed analysis of the resultant polymers. Following our mechanistic findings, we were able to produce new materials such as triblock copolymers as well as higher molecular weight diblock copolymers whose amorphous and crystalline nature can be tuned.

■ RESULTS AND DISCUSSION

The mechanism for block copolymer synthesis has been divided into three sections (Figure 1). Part 1 focuses on the insertion polymerization of 1-hexene and ethylene with a "classic" palladium diimine at ambient temperatures (**2a**; Figure 2). Part 2 explores the photoinitiated radical polymerization of methyl (meth)acrylates. Part 3 investigates the photoinitiated "switch" which allows for the synthesis block copolymers. Subsequently, the scope of block copolymer

synthesis is explored with various monomers such as 1-hexene, ethylene, methyl (meth)acrylate, ethyl acrylate, and *n*-butyl acrylate, using either a benzhydryl-derived ligand or a binuclear palladium complex, which led to the generation of diblock copolymers including a crystalline PE segment and amorphous ABA triblock copolymers.

In part 1, the livingness of the coordination insertion polymerization was investigated at room temperature to determine the time frame in which the livingness of the polymerization is maintained. In part 2, radical and spin trapping experiments were performed to identify the palladium complexes susceptible to Pd−C bond homolysis via EPR, NMR, and MS analyses. In part 3, photolysis of a Pd−C bond to generate a polyolefin macroradical was investigated as well with radical and spin trapping experiments via EPR, NMR, and MS analyses. Finally, a key intermediate is identified which plays a critical role in linking coordination insertion to radical polymerization. This mechanistic transition was successfully applied to facilitate di- and triblock copolymer syntheses including ethylene and α-olefins as well as acrylic and meth(acrylic) monomers.

Part 1: Insertion Polymerization. Insertion polymerization was used to polymerize α-olefins and ethylene and operates through a chain-walking mechanism[6a,b] consisting of three main processes beyond initiation: (1) chain propagation, (2) metal migration along the polymer chain, and (3) chain transfer.[6d,9] For our approach, we hypothesized that the palladium catalyst must be attached to the polymer chain for successful block copolymer synthesis; thus, particular attention was paid to the integrity of the catalyst during insertion polymerization. The livingness of Brookhart catalysis has been reported at low temperatures.[9,10] However, radical polymerization under these conditions is not ideal. As such, this work explores conditions at room temperature which favor living coordination insertion polymerization while being suitable for radical polymerization. We envision the livingness of coordination insertion polymerization depends on preventing chain transfer, which leads to the decomposition of the catalyst. To study the extent of chain transfer present in coordination insertion polymerization at ambient temperature, the evolution of molecular weight and conversion over time was monitored. While monitoring the reaction with ^{1}H NMR techniques, we observed that the polymerization continued to occur in aliquots, and therefore calculated conversions would be inaccurate. The conventional way to stop the polymerization is to quench the reaction with Et_3SiH. However, a significant overlap of the ethyl groups of Et_3SiH and the methyl groups of the polymers was observed in the ^{1}H NMR and led to inaccurate results. It is known that the addition of methyl acrylate to Brookhart catalysts significantly retards the rate of olefin insertion.[6d,9] Excess methyl acrylate was then adopted as an alternative additive to significantly slow the rate of propagation, thereby avoiding experimental errors. As a complementary technique to monitor conversion, we explored the use of *in situ* FTIR as a more direct method (section 4.1 in the Supporting Information).[11] *In situ* FTIR was applied to monitor real-time conversion with minimum invasion and results are in agreement with ^{1}H NMR of MA-doped aliquots (Figures S9 and S11). To our knowledge, this is the first use of this technique to monitor conversion for coordination insertion polymerization.

Dichloromethane (DCM) and chlorobenzene (PhCl) have been ubiquitously used in typical coordination insertion
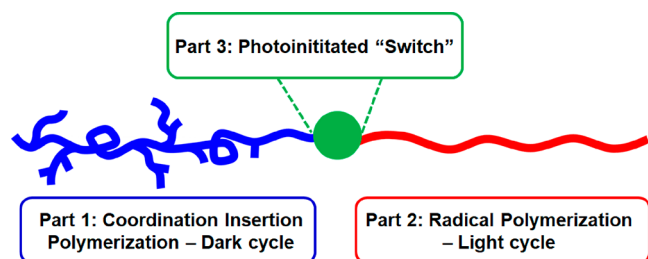

Figure 1. Outline of the mechanistic study for polyolefin−polar block copolymer synthesis in three separate parts.

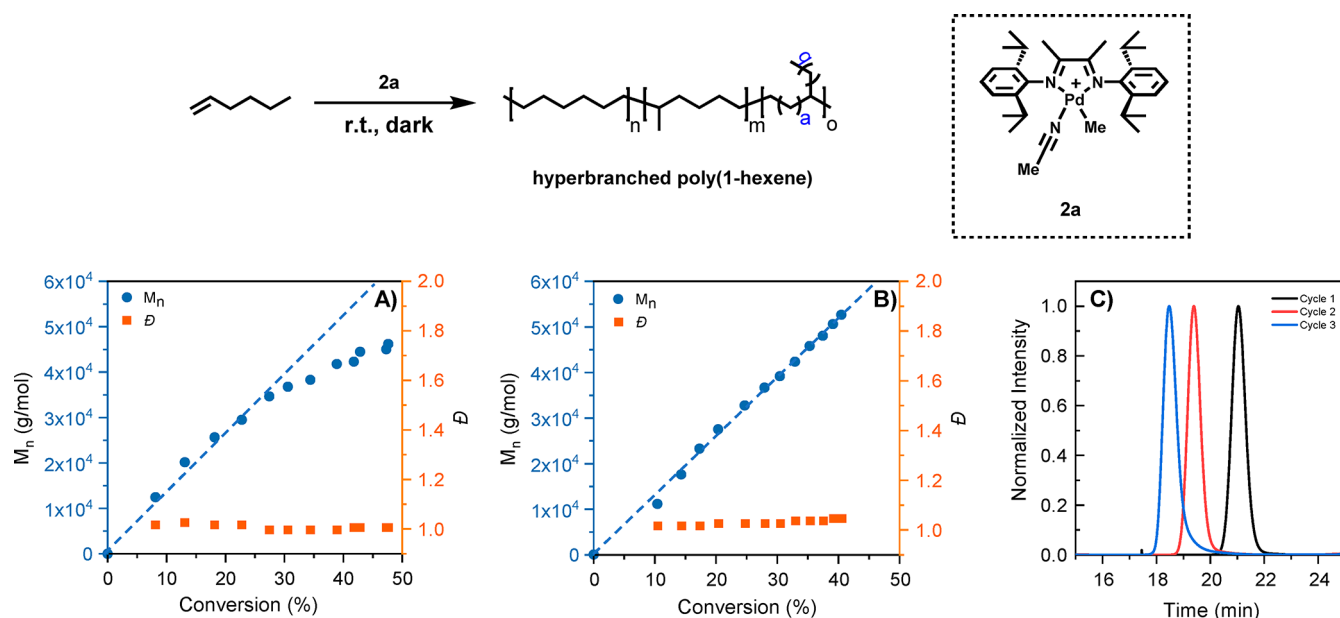hyperbranched poly(1-hexene)

2a

Figure 2. Coordination insertion polymerization of 1-hexene using catalyst **2a**. Molecular weight (blue) and polydispersity (orange) vs conversion graphs for polymerization reaction kinetics. (A) 1-Hexene polymerization in DCM. (B) 1-Hexene polymerization in PhCl. (C) SEC traces showing successive chain extensions from poly(1-hexene).

polymerizations for polar and nonpolar monomers and hence were chosen for these studies. For 1-hexene polymerization in DCM, a linear increase in molecular weight vs conversion was seen for the first 50 min of the polymerization (Figure 2a, Table S2, and Figures S9−S12). After 50 min, deviation from living behavior was observed, which is attributed to chain transfer and catalyst decomposition. In addition to chain transfer, isomerization was also detected over the course of the polymerization (Figures S9 and S12), which had a negligible effect on the chain growth of the polymer within the living time frame.[9] The behavior of the insertion polymerization in PhCl shows trends dissimilar to those seen with DCM (Figure 2B, Table S3, and Figures S14−S17). For polymerization in PhCl, a linear agreement between molecular weight and conversion was observed over a longer time frame in comparison to DCM. We attribute this observation to the ability of PhCl to compete for the fourth coordination site of palladium that is necessary for β-hydrogen elimination to occur and, in turn, reduce the rate of chain transfer.[12] Further investigation of the livingness of the coordination insertion polymerization at room temperature was established by chain extension studies. 1-Hexene polymerization was started and then stopped by the removal of the monomer under high vacuum. Fresh monomer was subsequently added to reinitiate the chain growth. The process was repeated twice and tracked *via in situ* FTIR (Figure S18) and GPC analysis (Figure 2C and Figure S19). The livingness was evidenced by the increase in molecular weight of the pre-existing polymers while narrow polydispersity was maintained (Đ < 1.1). Seeking to expand the scope to more industrially relevant monomers such as ethylene, we studied the livingness of ethylene polymerization at room temperature. Employing a approach similar to that for the 1-hexene study, the living time frame was determined to be 30 min in PhCl at room temperature (Table S10 and Figure S35). Taken together, these results establish conditions which are suitable for coordination insertion polymerization at room temperature.

Part 2: Radical Polymerization. Conflicting reports exist on the ability and inability of complex **2a** to initiate radical polymerization. Espinet et al. reported that **2a** does not initiate radical polymerization. However, Ye et al. reported that **2a** only initiates radical polymerization upon the addition of a small amount of norbornene. Additional studies have shown that light-promoted metal to ligand charge transfer is necessary for radical formation in palladium(II) species which produce alkyl radicals.[7e,13] We sought to shed more light on the reactive intermediates that play a role in the various steps of the radical polymerization. Although Brookhart-type Pd(II) complexes are reported to undergo radical polymerization, none of these works have focused on the mechanism through which this occurs.[7,14] A better understanding of the mechanism by which these complexes facilitate photoinitiated radical polymerization is paramount in our investigation probing the transformation from coordination insertion polymerization to radical polymerization. A combination of radical trapping experiments with TEMPO, spin trapping with EPR, and MS were used to characterize intermediates responsible for radical generation. These approaches together create a fundamental understanding of the photoinitiated radical polymerization involving the Brookhart-type complexes.

Identity of Radical Species and Mechanism of Radical Generation. In an effort to ascertain the identity of the generated radical species, **2a** was photolyzed in the presence of TEMPO acting as a suitable radical trap (Figure 3A). The resultant products from the reaction of **2a** and TEMPO has been fully characterized by NMR (Figure S37). As the reaction progressed, NMR analysis showed the gradual disappearance of the methyl peak attached to Pd(II) at 0.51 ppm and the development of a singlet at 3.59 ppm which corresponds to TEMPO-*Me*(**2**). Additionally, downfield shifts of isopropyl methine resonances from 2.86−2.90 to 3.11−3.20 ppm suggested the formation of a new Pd α-diimine species in which asymmetry is introduced. MS data pointed toward a three-membered-ring Pd−N−O species, which was later
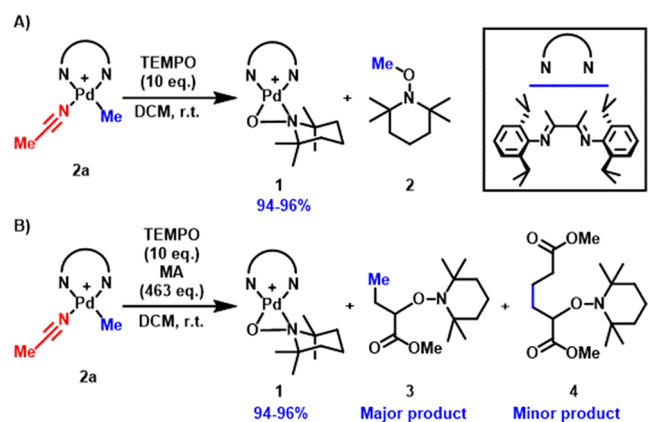
Figure 3. (A) Radical trapping of cation palladium diimine and methyl radicals with TEMPO. (B) Radical trapping of cation palladium diimine and methyl acrylate radicals with TEMPO.

confirmed by X-ray single-crystal diffraction analysis (Figure 4). The TEMPO-*Me* adduct **2** was isolated by column
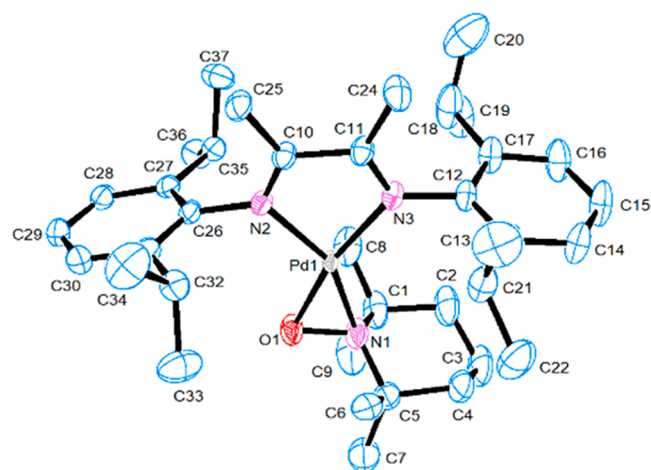

Figure 4. ORTEP diagram of Pd(II)-TEMPO adduct **1**. Hydrogen atoms and the BArF counterion are omitted for clarity. Selected interatomic distances (Å) and angles (deg): Pd1−O1 1.978(1); Pd1−N1 2.072(2); N1−O1 1.366 (2); Pd1−N2 2.043(1); Pd1−N3 2.081(2); N2−Pd1−O1 39.33(6); N1−Pd1−N2 154.03(6); N1−Pd1−N3 128.75(6).

chromatography and characterized by ^{1}H NMR and ^{13}C NMR (Figure S35). From these results, it was concluded that Pd−C bond homolysis generates an intermediary diimine Pd(I) radical which is then trapped by TEMPO, yielding adduct **1**. Simultaneously, the methyl radical is trapped by TEMPO to form adduct **2**.

Similar radical trapping experiments were carried out with **2a**, MA, and TEMPO to determine the identity of the radical initiator of polymerization (Figure 3B). The photolysis of **2a** in the presence of MA and TEMPO produced adduct **1** in a similar yield. It is noteworthy that the rate of Pd−C bond fragmentation in the presence of MA is faster in a more coordinating solvent such as PhCl in comparison to DCM, whereas the rate for the complex alone showed no significant differences (Figures S38 and S41). ESI-MS and ^{1}H NMR analyses of the crude reaction mixture also suggested the generation of a Me-MA-TEMPO adduct (**3**) and dimethyl heptanedioate-TEMPO (DMH-TEMPO) adduct (**4**) in a ratio

of 8:1 (Figure S40). These adducts were isolated by column chromatography and fully characterized by NMR (Figures S42 and S43). Surprisingly, adduct **2** was not observed in this radical trapping experiment. On the basis of this outcome, one conceivable pathway for the formation of **3** is through the photoinduced Pd−*Me* bond homolysis, and the resultant *Me* radical starts to propagate along one MA unit before being quenched by TEMPO. However, previous mechanistic studies revealed that migratory insertion of electron-deficient MA into the Pd−C bond occurs rapidly in a 2,1-fashion to form a four-coordinate intermediate which subsequently undergoes chain walking and rearrangement to a stable six-membered chelate.[6c,d,15] Additionally, compound **4** rules out methyl radicals having been the initiating radicals, as the dimeric acrylate complex arises from insertion of two acrylate monomers into the palladium complex, as observed by Brookhart et al.[6d] This proposes a more plausible scenario by which coordination insertion of MA into the complex precedes Pd−C bond homolysis.[6c] The MA-inserted species could cleave in the light to react with TEMPO immediately, yielding **3**, which is the dominant product evidenced by ^{1}H NMR analysis. The minor product **4** reflects the dimerization that occurs when a second MA inserts into the palladium complex, which can then cleave in the light subsequently followed by trapping with TEMPO (Scheme S1). ^{1}H NMR spectrum of the reaction prior to irradiation (t = 0 min) of the reaction mixture with MA monomer showed quantitative conversion of **2a** to the **2a**-MA-chelate complex, denoted by the disappearance of the Pd−CH_3 peak at 0.51 ppm and formation of the Pd−CH_2−CH_2 peak as a pentet at 0.66 ppm (Figure S40). This is in agreement with the mechanistic studies reporting the fast insertion of MA into the cationic palladium complex.[6d] This observation coupled with the absence of adduct **2** speaks against CH_3 radical generation in the presence of MA and instead indicates that insertion of MA precedes radical generation in the mechanism.

To confirm that insertion precedes radical generation, the **2a**-MA-chelate complex was synthesized and then subjected to photolysis in the presence of TEMPO (Figure 5). Surprisingly,
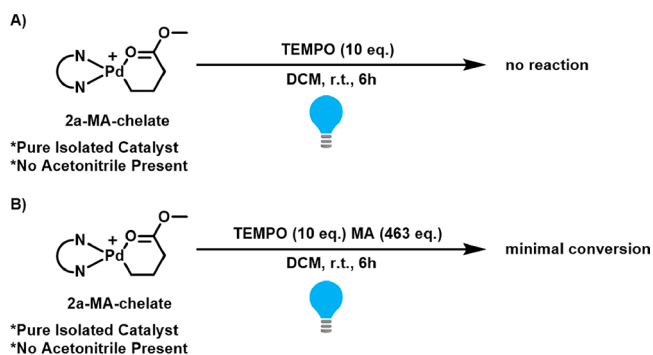

Figure 5. (A) Radical trapping of **2a**-MA-chelate with TEMPO. (B) Radical trapping of **2a**-MA-chelate with TEMPO and MA.

minimal conversion (<1%) was observed in the light over 3 h, in both the presence and absence of MA (Figure S44), which is in conflict with the result obtained when **2a** was used. This suggests that the chelate complex alone is ineffective at generating radicals to initiate a radical polymerization. As such, we hypothesized that the chelate must be opened for the effective homolysis of the Pd−C bond to take place. To assess

this, the radical trapping experiment with the **2a**-MA-chelate was performed with 1 equiv of acetonitrile (ACN) as an additive. The rate of Pd(II)-TEMPO formation in this reaction was comparable to the rate of photolysis of the **2a** complex (Tables S12 and S13). To gain insight into anticipated pathways for the radical generation, radical trapping experiments were conducted with different amounts of ACN with respect to the chelate complex. Kinetic studies showed that the conversion rate of **2a**-MA-chelate increased proportionately with the amount of ACN added, indicating that the ancillary ligand plays a crucial role in the photoinitiation step (Figures S47 and S48). In terms of radical generation efficiency, the quantum yield for the photolysis of complex **2a** in the presence of MA was determined to be much lower ($\Phi = 0.25$) than that of **2a** in the absence of MA ($\Phi = 0.86$) (section 5.8 in the Supporting Information). Furthermore, the rate of photolysis in the presence of MA ($\kappa = 0.0039$) is lower in comparison to the photolysis without MA ($\kappa = 0.0104$) (Figures S38 and S41). These observations taken together suggest that the lower photolysis efficiency observed can be attributed to the enhanced stability of the chelate complex compared to that of just **2a**.[15] Special attention is drawn to these results, as they confirm that a methyl radical is not the initiating species responsible for radical polymerization under the typical conditions; rather, an alkyl radical is generated through photolysis of the open form of the chelate.

To further understand the role that ligand binding strength has on Pd—C bond homolysis, the photolysis of the **2a**-MA-chelate complex under blue light was examined in the presence of TEMPO and different coordinating ligands in the same time frame of 18 h (Figure S42). Adding excess methyl propionate, a nonpolymerizing analogue of MA, resulted in a 45−49% conversion of the chelate complex to Pd(II)-TEMPO adduct **1**. The lower conversion in comparison to MA (89%, Figure S44) under the same conditions can be understood by the difference of available coordinating sites in each analogous compound. Additionally, when a stronger and sterically less bulky donor such as acetonitrile was used, full conversion was obtained within the same reaction conditions. These studies highlight that the efficiency of homolysis is proportional to the rate of chelate opening. Building on our hypothesis that chelate opening is required for Pd—C bond homolysis to occur, structures of adduct **3** and **4** from TEMPO trapping studies would suggest that chain walking is also required so that radical generation takes place at the position α to the carbonyl group. To investigate this, the photolysis of complex **2a** in the presence of TEMPO and MMA was investigated (Figure 6). It is known that the reaction of MMA with **2a** proceeds slowly via 1,2-insertion to yield a five-membered-ring chelate.[16] Due to this 1,2-insertion of MMA, the chelate formed upon reacting with **2a** has no β-hydrogens and leads to a resting state which is incapable of further chain walking. This unique chelation process was utilized to evaluate the role of chain walking in radical generation. The photolysis experiment's crude ^{1}H NMR spectra showed the complete conversion of **2a** into adduct **1** and the MMA-inserted chelate complex **11** in a ratio of 1.95:1 by the end of the reaction. The TEMPO-*Me* adduct **2** was also found and isolated from the reaction mixture. In addition, the isolated MMA-inserted chelate complex **11** was prepared and was subjected to TEMPO trapping experiments in the presence and absence of MMA monomers. Interestingly, no conversion was observed in either case (Figure S65). From these studies, it is understood that the Pd—C bond of complex
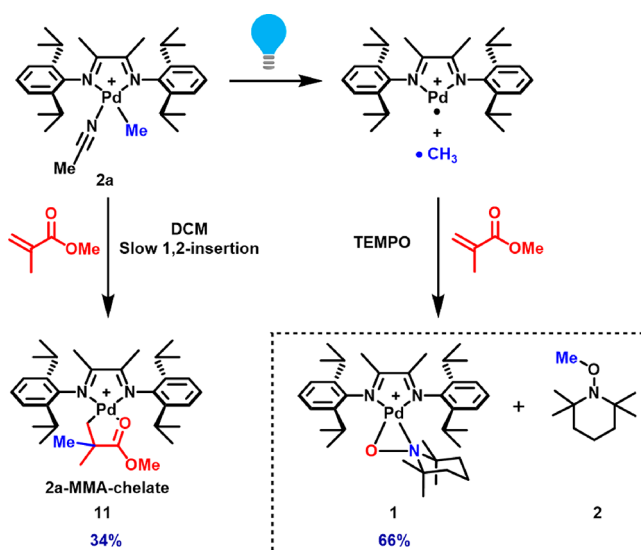

Figure 6. Radical trapping of palladium and methyl radicals with TEMPO in the presence of MMA.

2a, and not the **2a**-MMA-chelate, breaks to form Pd(I) radical species together with a methyl radical which initiates the homopolymerization of MMA through free radical polymerization. The importance of chain walking is solidified, as the lack of β-hydrogens for the MMA chelate prevents access to the carbon α to the carbonyl. The proposed mechanism confirms the requisite of β-hydrogen in the chelate complex, which facilitates chain walking to the labile intermediate (Figure 7).

Electron paramagnetic resonance (EPR) spectroscopy in combination with ESI-MS was used to directly observe and confirm the presence and structure of the initiating free radicals generated during photolysis of **2a** with and without monomer present. The advantage of this technique is the ability to detect radicals at very low concentrations.[17] Spin-trapping experiments were performed with **2a** and excess α-phenyl-*N-tert*-butylnitrone (PBN) in PhCl (Figure S49). When the mixture was irradiated with blue light, a distinct EPR resonance corresponding to the nitroxyl radical was detected. Modeling of the experimental spectrum suggests the reaction mixture comprises a Me-PBN spin adduct with coupling constants of $a_H = 3.43$ G and $a_N = 14.92$ G. FTMS was also performed for the reaction, and the Me-PBN adduct was observed at $[M + H] = 192.1374$ (Figure S52). Additionally, when this experiment was conducted in the presence of MA, a similar nitroxyl radical was the main EPR resonance observed and is consistent with an alkyl-PBN spin adduct (Figure 8). Me-PBN was not found though FTMS spectra, and this supports our understanding that *Me* radicals are not generated in the presence of MA. Spin trapping experiments were also performed with the **2a**-MA-chelate in the presence of PBN and ACN. FTMS for this experiment showed the presence of *Me*-MA-PBN at $[M + H] = 278.1748$ (Figure S54). The EPR and ESI-MS data again confirm that the opening of the chelate in blue light leads to the photolysis of the Pd—C bond, as witnessed by the presence of the *Me*-MA-PBN species. Throughout the EPR experiments, no spectral features attributed to Pd(I) species were observed, which is similar to previously reported EPR analyses of reactions that proceed through Pd—C bond homolysis.[18] This phenomenon may be due to the poor nucleophilicity of the putative Pd center
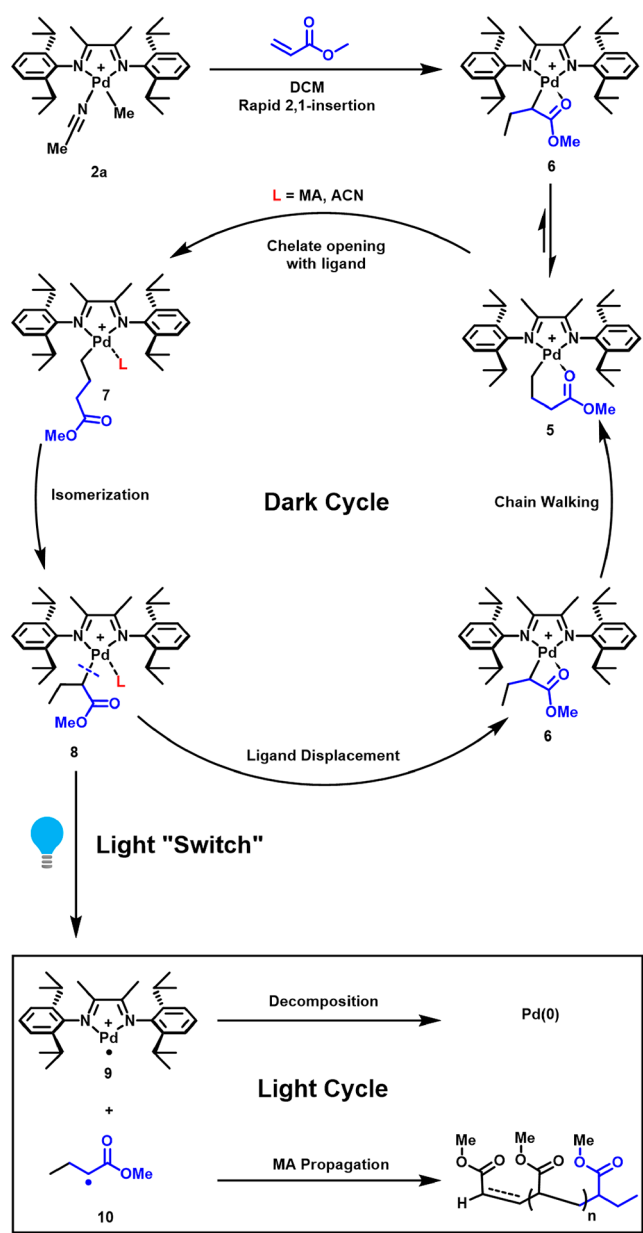
Figure 7. Proposed mechanism for the major pathway of radical polymerization of MA using palladium diimine complexes.

Figure 8. CW X-band (9.5 MHz, rt) EPR spectra of the trapped radical from the irradiated reaction mixture of **2a** in the presence of MA and PBN. A nonirradiated reaction mixture is shown in the control experiment.

radical in comparison to alkyl radicals and the relatively short lifetime of the Pd(I) species.

These results together with the structures of isolated compounds **3** strongly suggest the major mechanistic pathway for light-initiated radical polymerization of MA, as shown in Figure 7. Displacement of ACN in complex **2a** followed by rapid 2,1-insertion in an excess amount of MA yields **6**. Subsequent chain walking generates the stable chelate complex **5**, which is not susceptible to fragmentation under blue light. In the presence of ancillary ligands, **6** exhibits in equilibrium with **5** via the classical β-hydride elimination/reinsertion pathway. The intermediate **8** undergoes photodriven Pd−C bond homolytic cleavage to generate the reactive radical **10**, which is able to facilitate the free radical polymerization of MA (section 5.9 in the Supporting Information). The cationic Pd(I) radical species is not stable and further decomposes to form Pd black. The termination pathway of light-initiated
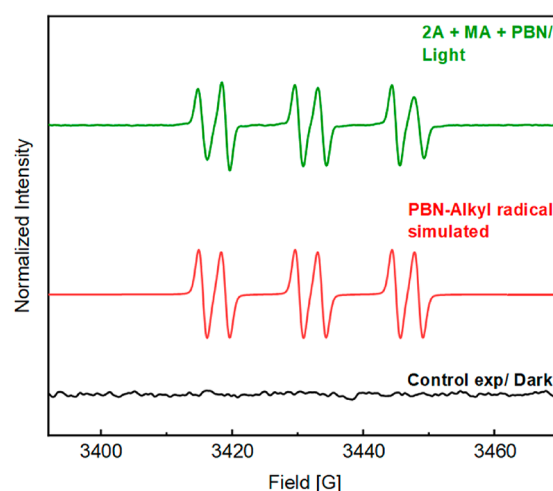
radical polymerization was also investigated using NMR, MS, and MALDI-Tof (section 5.10 in the Supporting Information). Conventional free radical polymerization is usually conducted at an elevated temperature that yields high-molecular-weight polyacrylates. However, the chain growth can be significantly hampered by increasing the amount of photoinitiator (which is complex **2a** herein) while lowering monomer concentration and maintaining the low temperature (25 °C).[19] As such, this method produced a short PMA polymer (~2000 g/mol). ^{1}H NMR and ESI-MS spectra of the reaction showed a mixture of unreacted **2a**-MA-chelate and PMA (Figures S61 and 62). MALDI-ToF of the polymers reveals a series of peaks that were separated by one MA unit (m/z 86.04). Each peak's isotopic distribution was found to be identical with the simulated distribution of a 1:1 mixture of PMA with saturated and unsaturated chain ends (Figure S63). These data, coupled with the olefinic resonances observed in ^{1}H NMR, suggests that the termination pathway proceeds through a disproportionation mechanism. This is in good agreement with previous reports of Coote and Yamago for the radical polymerization of MA.[20] With an understanding of both the coordination insertion polymerization along with our new insights into the mechanism responsible for the radical polymerization, the "switch" between theses platforms was then investigated.

Part 3: Photoinitiated "Switch": Radical Generation from the Polyolefin. Following insights gained from the mechanistic studies of both polymerization pathways, the mechanism by which an active radical can be generated at the polyolefin chain end was investigated. It has been well established that adding MA to the 1-hexene polymerization results in the rapid formation of the six-membered-ring chelate complex, which impedes further propagation.[6c,d,21] On the basis of previous studies discussed above, we hypothesized that the opening of the chelate followed by photolysis of the Pd−C bond produces a polyolefin macroradical, allowing for an irreversible switch from insertion to radical polymerization. In this section, we present experiments geared toward a better understanding of radical generation from the polyolefin.

Synthesis and Characterization of Polyolefin Macro-chelate, the Key Intermediate. *In situ* formation of the macrochelate presents challenges for directly characterizing the

radical generation, and as such, developing novel synthetic methods for these reaction intermediates was necessary. The synthesis of the Pd-poly(1-hexene)-MA chelate is performed by reacting catalyst **2a** with 1-hexene and MA, followed by careful removal of all volatiles to obtain a stable macrochelate (section 6.1 in the Supporting Information). Characterization of the macrochelate was performed using NMR (Figure S68–S78) and ESI-MS analyses (Figure S67). ^{1}H DOSY NMR confirmed the connectivity of the Pd species to the poly(1-hexene) chains, indicating no unbound palladium catalysts (Figure 9).
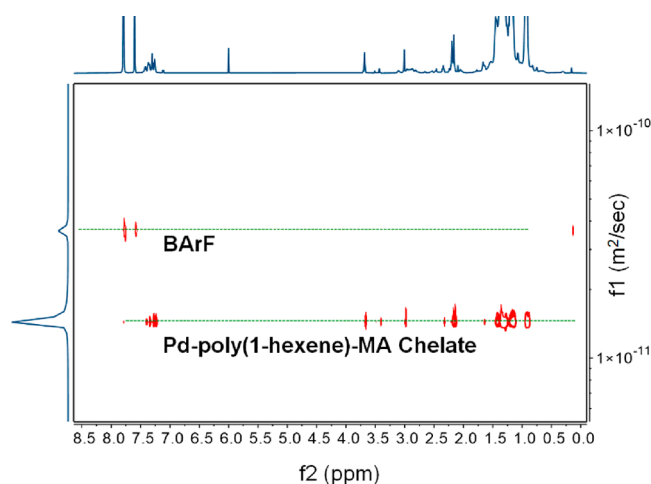

Figure 9. ^{1}H DOSY NMR (600 MHz, TCE-d_2, 298 K) spectra of the Pd-poly(1-hexene)-MA chelate. The resonances corresponding to the palladium complex and the polyolefin show similar diffusion behavior. The diffusion behavior of the BArF is indicative of a weakly coordinating counterion.

ESI-MS shows a narrow poly(1-hexene) distribution bearing one MA unit and the palladium moiety, where each peak exhibits a palladium isotopic pattern. Interestingly, 1-D and 2-D NMR suggests a variety of conformations that exist for the synthesized macrochelates, similar to the structure of the **2a**-MA-chelate. Pd-polyethylene(PE)-MA chelate samples were prepared and characterized similarly to the Pd-poly(1-hexene)-MA macrochelates (section 6.2 in the Supporting Information). Pd-PE-MA chelate samples show a similar narrow distribution bearing one MA unit and the palladium moiety (Figure S81). Once we identified the structure of the macrochelates, they were then used to probe the switch mechanism that allows for the formation of block copolymers.

Spin Trapping Analysis of the "Switch". First, we investigated the identity of radical species generated from the macrochelates using EPR studies established in the radical section. As aforementioned, before the "switch", a Pd-poly(1-hexene)-MA chelate was formed and fully characterized. Next, a macrochelate with a molecular weight of 2.8 kDa was subjected to EPR experiments in the absence and presence of MA monomers and ACN (Figure S90). A triplet of doublets was observed in the recorded spectra, which is consistent with a well-known PBN trapped alkyl radical with coupling constants of $a_H = 2.79$ G and $a_N = 14.65$ G.[22] In support of the EPR results, the high mass region of the FTMS spectra shows a distribution of poly(1-hexene)-PBN adducts differing by one 1-hexene mass unit (Figure S91). In addition to these observations, no signal was observed in the dark, which highly

suggested that a carbon-centered radical generation was triggered by blue-light irradiation. The results from the EPR experiments confirm the generation of alkyl radicals from the macrochelates and strongly suggest that the alkyl radical is formed in the light-induced "switch" process. Having confirmed the generation of the alkyl radical, we next studied the location of the bond homolysis in the macrochelate using radical trapping methods.

Radical Trapping Characterization of the "Switch". As it has already been shown that TEMPO is effective in capturing the alkyl radical generated in the light cycle (Figure 4), similar photolysis experiments were performed using the Pd-poly(1-hexene)-MA and Pd-PE-MA macrochelates (sections 6.4 and 6.5 in the Supporting Information). ESI-MS shows a loss of the palladium moiety ($C_{28}H_{40}N_2Pd$, 510.22 Da), and the addition of TEMPO ($C_9H_{18}NO$, 156.14 Da) accounts for an overall loss in mass of 354.08 Da (Figures S69 and S93). This observation suggests that the palladium chelate is formed and attached to the polymer chain, and photolysis of the Pd–C bond results in the formation of the polyolefin-TEMPO adduct (Figure 10). From these results, the location of radical
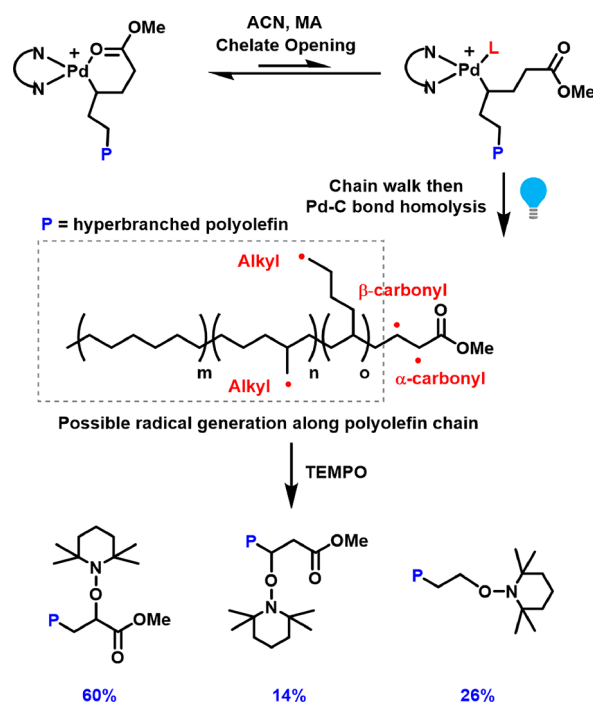

Figure 10. Radical trapping experiments with a Pd-(1-hexene)-MA chelate in the presence of TEMPO. Relative percentages of poly(1-hexene)-TEMPO adducts were determined by quantitative ^{13}C NMR.

generation along the polyolefin chains was probed via a series of NMR experiments (^{1}H, ^{13}C, ^{1}H–^{13}C HSQC and HMBC, ^{1}H–^{15}N HMBC) (Figures S94–S99). ^{1}H NMR analysis shows resonances in the region from 4.15 to 4.30 ppm, which corresponds to the methine proton α to the carbonyl where the TEMPO is attached. The quantitative ^{13}C NMR spectra of the sample exhibit C–H resonances from 84.5 to 86.5 ppm, which correspond to methine carbons attached to which are α to the carbonyl (60%). Another C–H resonance is located at 82.0 ppm, which corresponds to methine carbons attached to the oxygen of TEMPO which is β to the carbonyl (14%). C–H$_2$ resonances from 76.5 to 81.5 correspond to methylene carbons where the TEMPO is attached at the end of the butyl

or methyl branch (26%). $^1H-^{15}N$ HMBC is also applicable to these unique structures and was used to identify a three-bond correlation between the polymeric hydrogen α to the nitrogen through the oxygen of the TEMPO moiety, confirming their connectivity (Figure 11). Additional 2-D NMR experiments were employed to further confirm the identity of the TEMPO adducts.
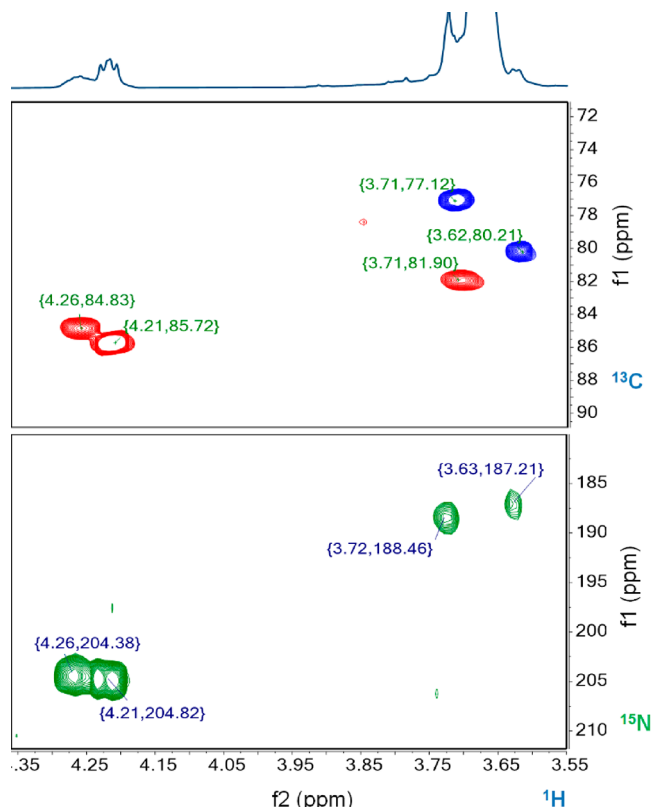

Figure 11. (top) $^1H-^{13}C$ phase edited HSQC (600 MHz, TCE-d_2, 298 K) of poly(1-hexene)-TEMPO adducts (methine shown in red, methylene shown in blue). (bottom) $^1H-^{15}N$ gHMBC (600 MHz, TCE-d_2, 298 K) of poly(1-hexene)-TEMPO. Both spectra highlight the connectivity between the polymer and the TEMPO moiety.

The TEMPO-trapped polymers are a result of the chain-walking nature of the palladium, which allows the palladium to chain walk to the α carbonyl when the chelate is opened. All structures also contain only one TEMPO trapped unit per chain, confirming that, for every polymer chain bearing the catalyst, only one alkyl radical is produced. This explains why diblock copolymers are selectively formed through this pathway. The key mechanistic features of the polymerization which allow for polyolefin macroradical generation are as follows (Figure 12). First, the addition of methyl acrylate to a growing polyolefin chain rapidly inserts and forms a Pd-polyolefin-MA chelate. The opening of the chelate promotes chain walking α to the carbonyl,[14] where Pd−C bond homolytic cleavage occurs under blue light, generating a carbonyl-stabilized macroradical. To a lesser extent, chain walking to the end of the nearest branch followed by Pd−C bond homolysis generates other alkyl macroradicals. The distribution of trapped alkyl radicals observed can be explained by the resting state of the Pd(II)-alkyl complex during chain walking, in which Pd-n-alkyl is more thermodynamically favorable than Pd-iso-alkyl.[23] The enhanced stability of the chelate allows for the continuous generation of free radicals at a low concentration, which is an essential requirement in free radical polymerization techniques.[24] The ability to initiate radicals from a single site along a polyolefin chain was then applied to the synthesis of block copolymers.

Scope of MILRad Polymerization: Polyolefin−Polar Block Copolymer Synthesis and Characterization. The main takeaway from the mechanistic investigations is summarized as follows with regard to block copolymer synthesis. Macroradical formation requires homolysis between the Pd−C bond where the palladium is attached to the polyolefin. Therefore, living conditions were used for the insertion coordination polymerization, ensuring that each polymer chain was bound to palladium. Conditions that avoid decomposition of the Pd complex are necessary to maintain access to the macroradicals. Furthermore, conditions which prevent formation of Pd-hydride via chain transfer are vital, as MA insertion and subsequent photolysis from the hydride species can generate homopolymers. The implementation of these key mechanistic findings results in a robust methodology that facilitates access to a variety of polyolefin−
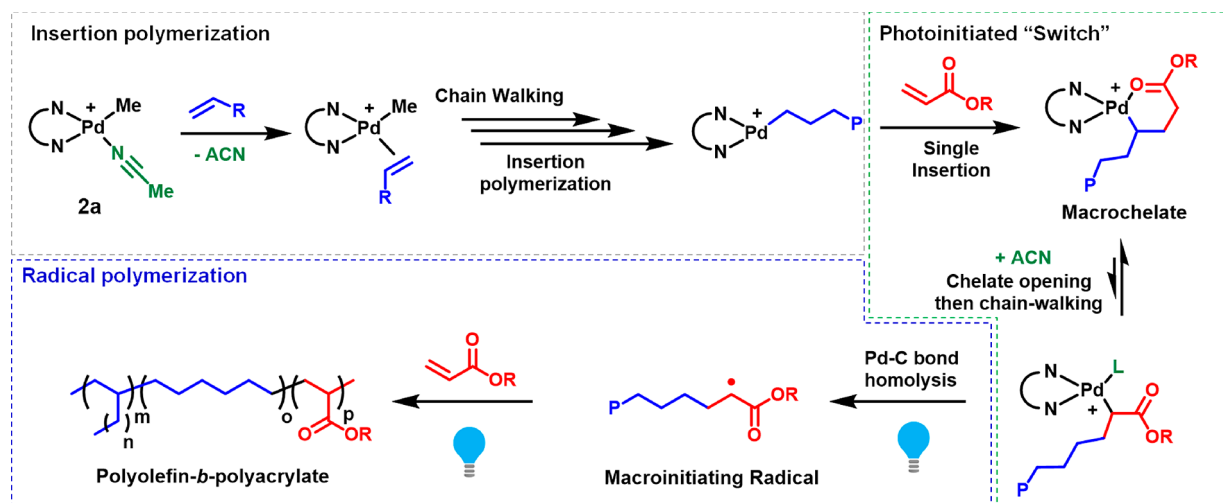

Figure 12. Proposed mechanism for polyolefin−polar block copolymer formation.

polar block copolymers. This section culminates in a broad range of polyolefin–polar di- and triblock copolymers with different compositions now available in light of the mechanistic studies (Figure 13). As polyolefin-*b*-polyacrylate polymers
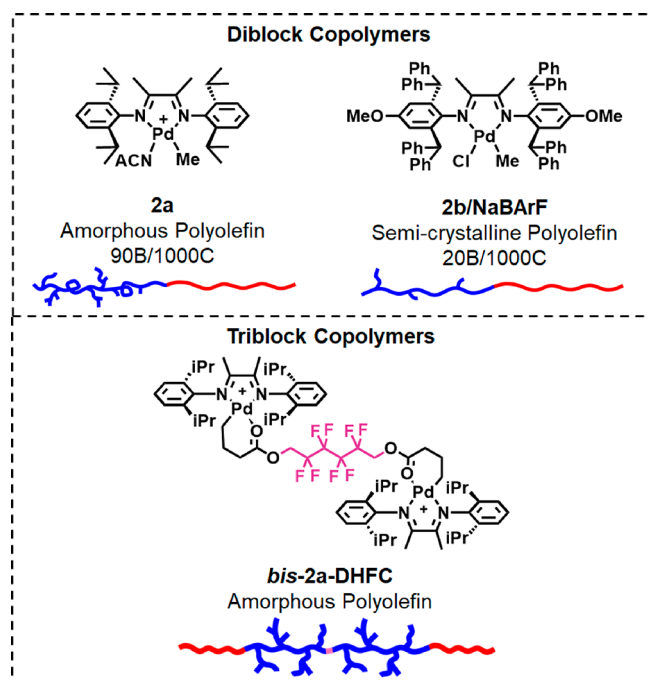

Figure 13. Types of di- and triblock copolymers via MILRad polymerization described in this work (Table 1).

largely remain a rare and underexplored material platform, a complete characterization of the new materials was accomplished by employing a combination of characterization techniques such as MALDI-ToF, DOSY, SEC/GPC, small-angle X-ray scattering (SAXS), dynamic light scattering (DLS), transmission electron microscopy (TEM), and thermal analysis.

Diblock Copolymers Containing Amorphous Poly(1-hexene) (PH) Segments. *Matrix-Assisted Laser Desorption/Ionization-Time of Flight (MALDI-ToF).* Initially, short polyolefin–polar block copolymers were synthesized so that they could be characterized by MALDI-ToF, whose distribution would be indicative of block copolymer formation and also provide evidence as to the possibility of chain transfer. The Pd-poly(1-hexene)-MA chelate was employed for the synthesis of low-molecular-weight PH-*b*-PMA block copolymers. Photoinitiated radical polymerization of MA proceeded for 3 h and was then quenched with Et$_3$SiH. This time frame was chosen so that the composition of the reaction mixture would allow for characterization by MALDI-ToF. The spectra of the resultant polymer show two distributions in which the lower molecular weight distribution is the dominant species and was identified as a saturated poly(1-hexene) bearing a single MA unit (Figure S112). The origin of this low-molecular-weight polymer is understood to be the quenched product of the macrochelate. Unsaturated polyolefins, as a result of the chain transfer pathway, were not observed. This indicates that these conditions do not lead to the formation of small molecule palladium chelates, and thus the generation of PMA homopolymers is not possible under these conditions. In a second example, MA was allowed to react for 24 h, reaching

high conversion, and then the reaction mixture was quenched with Et$_3$SiH. The mass spectra revealed a main distribution corresponding to PH-*b*-PMA block copolymers (Figure S113). For example, the peak at *m/z* 2080 is assigned to block copolymers with a total DP = 24 (Figure 14, left). Within this
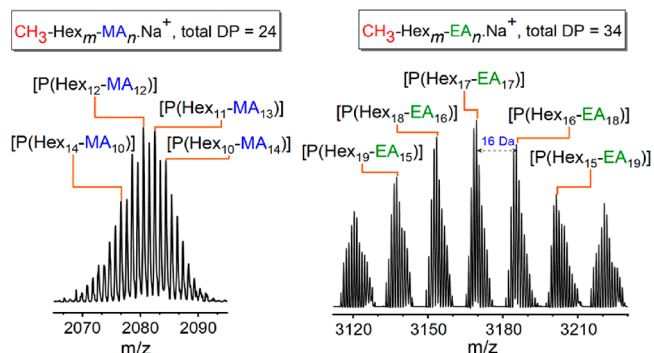

Figure 14. Expansion of the MALDI-ToF spectra of (left) PH-*b*-MA (Table 1, entry 1) and (right) PH-*b*-PEA (Table 1, entry 2), showing the comonomer distribution for DPs **24** and **34**.

cluster, PH$_{11}$-*b*-MA$_{13}$ and PH$_{12}$-*b*-MA$_{12}$ block copolymers with a masses of 2082.5 and 2080.6 Da were found, respectively. This small mass difference between block copolymer compositions (Δ = 2 Da) within similar DPs results in a significant signal overlap in the mass spectra (Figure S113b for complete assignment).[25] In order to obtain more resolved spectra, methyl acrylate was replaced with ethyl acrylate to create a higher difference in mass (Δ = 16 Da).[26] In this spectrum, a comonomer distribution of poly(1-hexene) and poly(ethyl acrylate) is seen within the range for a given total DP = 34 (Figure 14, right, and Figure S114).[27] The larger Δ value in this spectrum allows for better resolution that confirms the block structure of the polymers formed. Additionally, unsaturated and saturated chain ends were found in each peak cluster (Figures S113 and S114). This is consistent with results from MA homopolymerization in which termination undergoes disproportionation. This method for characterizing polyolefin–polar block copolymers is a powerful technique that has not been previously explored for these polymers.

Size-Exclusion Chromatography (SEC) and Purification of the Block Copolymers. Following short block copolymer syntheses, larger block copolymers were synthesized in a one-pot, sequential monomer addition manner with variations in the size of the polyolefin block. On the basis of our results from the insertion coordination polymerization, different length poly(1-hexene) blocks were synthesized within the living window for both PhCl and DCM by varying the time while keeping the concentration of **2a** constant. All polymerizations exhibited the same phenomenon throughout the reaction, as the photolysis of the Pd–C bond of the opened-form macrochelate generates macroradicals that initiate free radical polymerization of MA generating block copolymers. As evidenced from the GPC analysis of the crude reaction mixture, we observed a mixture of block copolymers and unreacted macrochelates (section 7 in the Supporting Information). The generation of macroradicals during the reaction produces palladium species that decompose to Pd black. The buildup of Pd black, witnessed by the darkening of the reaction mixture, prevents effective Pd–C bond photolysis for other macrochelates, as light penetration is drastically

Table 1. Selected Polyolefin-Polar Block Copolymers[h]

		Polyolefins					Polyolefin-*b*-polyacrylate			Thermal properties		
Entry	Sample	Macro-initiator	M_n (kg/mol)	Mw (kg/mol)	Đ	Co-monomers	M_n (kg/mol)	M_w (kg/mol)	Đ	T_g (°C)	T_m (°C)	T_c (°C)
1	PH-PMA[a,d]	PH	3.2	3.4	1.05	MA	5.1	6.8	1.33	ND	ND	ND
2	PH-PEA[a,d]	PH	2.6	2.7	1.05	EA	3.8	4.9	1.19	ND	ND	ND
3	PH-PMA[a,d]	PH	11.9	12.1	1.02	MA	78.6	139	1.77	-60/12	-	-
4	PH-PMA[a,d]	PH	31.6	33.3	1.05	MA	102	158	1.54	-60/12	-	-
5	PH-PMMA[a,d]	PH	25.4	26.4	1.04	MMA	103	195	1.26	-64/101	-	-
6	PE-PMA[a,d]	PE	29.7	30.7	1.03	MA	36.1	39.7	1.10	-66/12	-	-
7	PE-PMA[a,d,g]	PE	29.7	30.7	1.03	MA	85.4	126	1.47	-66/12	-	-
8	PE-PMA[a,e]	PE	22.7	23.5	1.04	MA	134	269	2.00	-66/12	-	-
9	PE-P(*n*BA)[b,f]	PE	43.7	50.9	1.16	n-BA	202	420	2.08	-54	106	71
10	PE-P(*n*BA)[b,f]	PE	43.3	50.8	1.17	n-BA	345	807	2.34	-54	104	66
11	PMA-PE-PMA[c,d]	PE	99.4	105	1.05	MA	319	511	1.60	-67/12	-	-

[a]Complex used for the syntheses: **2a**. [b]Complex used for the syntheses:**2b** activated *in situ* with 1.2 equiv of NaBArF. [c]Complex used for the syntheses: bis-**2a-DHFC**. [d]Molecular weight and polydispersity index (Đ) were determined by GPC analysis with samples run in THF at 40 °C calibrated to poly(methyl methacrylate) standards. [e]Molecular weight and polydispersity index (Đ) were determined by GPC analysis with samples run in CDCl₃ at 40 °C calibrated to poly(methyl methacrylate) standards. [f]Molecular weight and polydispersity index (Đ) were determined by GPC analysis with samples run in TCB at 150 °C calibrated to polystyrene standards. [g]Sunlight was used instead of blue light. [h]Samples correspond to polyolefin−polar block copolymers synthesized as described in the text with a variety of block compositions. Abbreviations: PH = poly(1-hexene), PE = poly(ethylene), PMA = poly(methyl acrylate), PEA = poly(ethyl acrylate), PMMA = poly(methyl methacrylate), P(*n*BA) = poly(*n*-butyl acrylate).

reduced throughout the reaction. To further confirm the nature of the unreacted polyolefin, block copolymer purification techniques were employed. Soxhlet extraction is a common technique for separating polymers on the basis of the variance in solubility exhibited between different polymers. It has been reported that this method was successful in separating a homopolymer mixture of polyethylene and poly(methyl methacrylate).[8b,28] Soxhlet extraction was ineffective at separating the block copolymer from the unreacted polyolefin, which is attributed to the aggregation properties of the block copolymer in a selective solvent (Figure S102). Dynamic light scattering (DLS) analysis reveals that micellization of the block copolymer produces sub-micrometer aggregates in both polar and nonpolar solvents which can travel through the pores of the extraction thimble (6 µm) (section 7.1.7 in the Supporting Information). If a mixture of pure homopolymers were generated, this method would have been successful. In light of this observation, alternative methods were developed to separate the polymer mixture. A centrifugation method was effective at removing unreacted polyolefins (detailed and validated in section 7.1.1 in the Supporting Information). This method takes advantage of the partial solubility of the block copolymer in comparison to the complete solubility of the polyolefin in nonpolar solvents at room temperature. The block copolymers can be recovered at high yield (∼80%) as pellets, whereas the supernatant contains the totality of unreacted polyolefins and a minority of block copolymers (Table S18 and Figure S103). ¹H NMR analysis of the separated polymers revealed that both spectra were absent of olefinic resonances (5.0−6.0 ppm), highlighting that chain transfer is absent under these synthetic conditions (Figure S116). The absence of chain transfer rules out the generation of Pd-hydride, which subsequently excludes a pathway for the formation of homopolymers. As a result, PHs with different

molecular weights (11−32 kDa) were prepared, and subsequent radical polymerization of MA yielded block copolymers with a molecular weight range of 60−101 kDa (Table 1, entries 3 and 4, and Table S18). As mentioned above, the insertion of MMA into the Pd−alkyl bond gives a complex inert toward light-induced radical polymerization. Consequently, light-induced block copolymerization with sequential addition of 1-hexene and MMA was not successful. However, by using a Pd-poly(1-hexene)-MA chelate as an intermediate, poly(1-hexene)-*b*-poly(methyl methacrylate) (PH-*b*-PMMA) block copolymers were accessible (Table 1, entry 5; detailed in section 7.1.3 in the Supporting Information).

Small-Angle X-ray Scattering (SAXS). The purified block copolymers were submitted for SAXS analysis, and all polymers exhibited principal scattering peaks, confirming the existence of block copolymer structures (section 7.1.6 in the Supporting Information). The interplanar spacing (calculated as *d* spacing = $2\pi/q*$) changes are most likely attributed to different molecular weights of each segment within the diblock copolymers.

Thermal Properties. The purified block copolymers and isolated polyolefins were subjected to differential scanning calorimetry (DSC) measurements. The DSC traces of the block copolymers exhibit two glass transition temperatures (T_g), which are in the range of poly(1-hexene) (−60 °C, broad) and poly(methyl acrylate) (11 °C), respectively (Figure S119a, left). This is indicative of block copolymers containing long block segments which are in heterogeneous phases.[29] The isolated polyolefin exhibits a single T_g value at −60 °C (broad), indicative of a homogeneous phase (Figure S119a, right).

Diblock Copolymers Containing Amorphous-PE or Crystalline-PE Segment. To further confirm the scope of

block copolymer polymerization with other monomers, blocks consisting of polyethylene-*b*-polyacrylate (PE-*b*-PMA and PE-*b*-PnBA) were synthesized. PE-*b*-PMA was synthesized by first conducting coordination insertion polymerization of an olefin and then generating the chelate by addition of MA. Following the synthesis of the macrochelate, MA monomers and 1.2 equiv of ACN were added in the presence of light to facilitate Pd−C bond photolysis, which produced the final block copolymers. The efficiency of light-induced generation of the polyolefin macroradical was also demonstrated by utilizing sunlight as opposed to blue LEDs (Table 1, entry 7). After 12 h irradiation by sunlight, a PE-*b*-PMA block copolymer with M_n = 85000 g/mol was successfully obtained from its Pd-PE-MA precursor. It should be noted that the conversion of MA monomer was found to be slower than that when blue light was used (Table S28). It is known that the classical Brookhart catalyst **2a** generates amorphous polyolefins as a result of the chain-walking mechanism. Thus, in order to explore the versatility of the Pd(II) diimine platform, catalyst **2b** was used to achieve semicrystalline PE blocks. Block copolymerization of ethylene and *n*-butyl acrylate (nBA) were performed in a one-pot, sequential addition fashion to generate semicrystalline polyolefin−polar block copolymers (section 7.2.2 in the Supporting Information). By variation of the amount of nBA monomer, different P(nBA) lengths were achieved (Table 1, entries 9 and 10). A comprehensive analysis by different techniques such as SAXS, DSC, NMR, and GPC again confirms the existence of block copolymer architectures for these materials (section 7.2.4−7.2.6 in the Supporting Information).

¹H Diffusion-Ordered NMR Spectroscopy (DOSY). For this study, PE-*b*-PMA (Table 1, entry 8) was selected and ¹H DOSY experiments were performed on both the crude sample and purified sample in which unreacted PE was removed. The 2D spectra of the crude polymer mixture shows two distinct resonances corresponding to the PE-*b*-PMA diblock copolymer and unreacted Pd-PE-MA chelate, which exhibited two diffusion coefficients (Figure 15, top). Following purification of the sample, a single resonance was obtained where the signals of PE (1.26−0.9 ppm) and PMA (3.65 ppm) were aligned at the same diffusion coefficients, confirming a block copolymer architecture (Figure 15, bottom).

Thermal Analysis. Similar to the PH-*b*-PMA materials, amorphous PE-*b*-PMA diblocks synthesized using **2a** exhibit two glass transition temperatures (T_g), corresponding to its homo polyethylene and homo polyMA segments, at −66 and 12 °C respectively (Figure S132). In contrast, due to its slow chain-walking properties, **2b** can generate PE with dramatically lower degree of branching (20 B/1000 C) as opposed to its classic version **2a** (90 B/1000 C) (Figures S129−S130).[30] As a result, the PE-*b*-P(nBA) block copolymers synthesized using **2b** exhibit melting points of more than 100 °C (Table 1, entries 9 and 10). In comparison to the homo polyethylene obtained from the same catalyst, a small reduction (1−3 °C) in melting temperatures of these materials was observed. However, the addition of the P(nBA) segment led to a significant drop in crystallization temperature in the cooling cycles (Figure S133). This phenomenon is usually observed in crystalline−amorphous (C-A) diblock copolymers, which is caused by the perturbation of amorphous blocks in the nucleation, chain folding, and orientation of the crystallizable segment.[31]
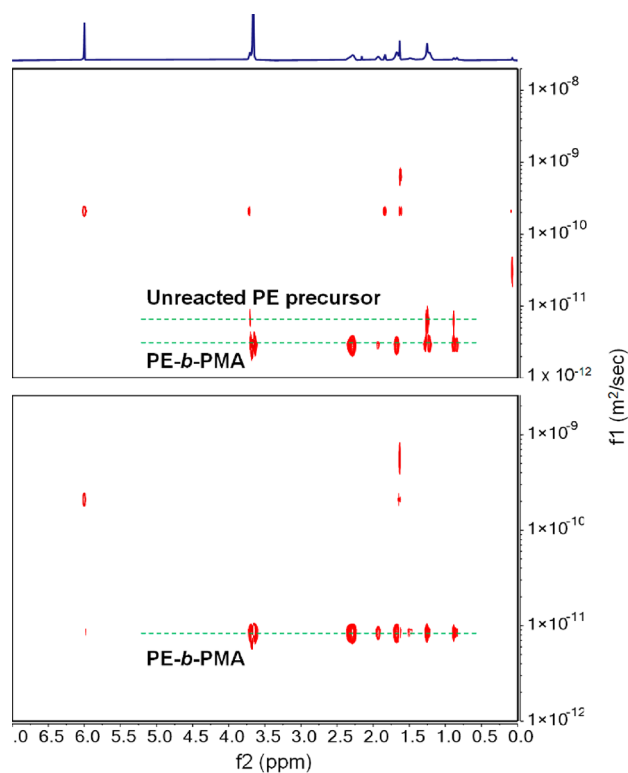

Figure 15. ¹H DOSY NMR (600 MHz, TCE-d_2, 298 K): (top) mixture of unreacted PE precursor and PE-*b*-PMA; (bottom) purified PE-*b*-PMA. The resonances corresponding to the PE block and the PMA block show similar diffusion behavior.

Aggregation Behavior. Amphiphilic block copolymers are known for their ability to self-assemble into micelles in a selective solvent (Figure 16). PE-*b*-P(nBA) (Table 1, entry 9)
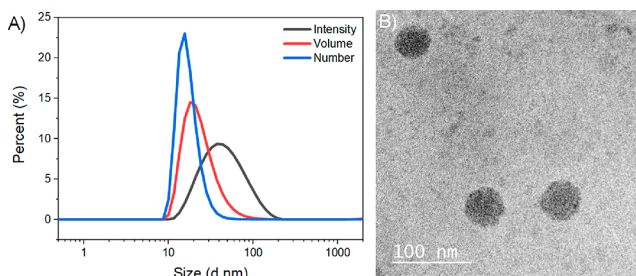

Figure 16. Micellization of PE-*b*-P(nBA) (Table 1, entry 9) block copolymer in THF confirmed by DLS analysis and TEM imaging. The average diameter was estimated to be ∼42 nm.

was found to create a clear solution at a concentration of 1 mg/mL in THF, and this sample was analyzed by both dynamic light scattering (DLS) and transmission electron microscopy (TEM) (Figure 16). Correlogram and size distribution histograms can be found in section 7.2.7 in the Supporting Information.

Triblock Copolymer PMA-*b*-PE-*b*-PMA. In comparison to diblock copolymers, triblock copolymers exhibit a superior property as compatibilizers for polymer blends and many other applications.[3a] However, the preparation of triblock copolymers combining PE and polar blocks remains a great challenge. The common strategy to access these types of materials is through telechelic polyolefins bearing suitable functional groups for the subsequent polymerization.[32] Mechanistic

insights into this study revealed that the Pd−C bond of the **2a**-MA-chelate complex can be homolyzed under blue light when this is assisted by opening of the chelate by an ancillary ligand. This chelate is also capable of polymerizing ethylene in a living fashion under suitable conditions.[10] With this in mind, we developed a binuclear Pd(II) complex (*bis*-**2a**-DHFC) bearing a 1,6-bis(acryloyloxy)-2,2,3,3,4,4,5,5-octafluorohexane linkage (detailed synthesis and characterization can be found in section 3.5 in the Supporting Information). This strong electron-withdrawing linker was carefully selected to ensure fast initiation and, as a result, a uniform chain growth from both metal centers.[6c] This complex is stable for weeks at −30 °C under inert conditions even though its mono analogue, Pd-fluorinated octyl acrylate (FOA) chelate complex, was found to be unstable and decomposed with time and handling.[6c] The structure of the complex was verified by single-crystal X-ray diffraction analysis (Figure 17). The livingness of ethylene
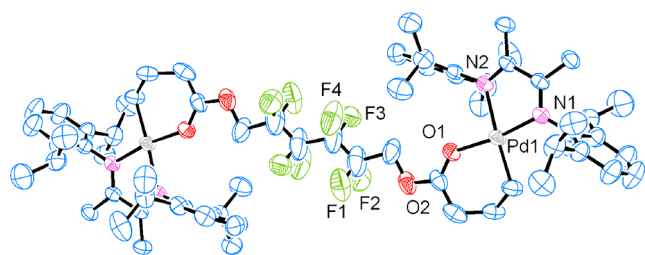

Figure 17. ORTEP diagram of the bis-**2a**-DHFC complex. Hydrogen atoms and BArF counterions are omitted for clarity.

polymerization catalyzed by bis-**2a**-DHFC was investigated through kinetic studies (section 8.1 in the Supporting Information). During the course of the reaction, the polymerization exhibited a linear increase in molecular weight over time while maintaining narrow polydispersity ($Đ$ = 1.03−1.11), which indicates a high level of controlled polymerization with negligible chain transfer (Table S30 and Figure S137a,b). To the best of our knowledge, this is one of the rare examples of binuclear palladium catalysts that can achieve this narrow molecular weight distribution ($Đ$ > 1.46 for other catalysts).[33] ^{1}H NMR analysis of the obtained PE in chloroform-*d* showed the distinctive peak of COOCH_2CF$_2$ at 4.76 ppm, suggesting the attachment of the fluorinated ester linkage. As evidence of simultaneous chain growth, the obtained PE was subjected to a hydrolysis experiment. The hydrolyzed products exhibit a single peak whose molecular weight is half that of the parent species, and a ^{1}H NMR spectrum of the species showed the disappearance of the COOCH_2CF$_2$ peak (Table S30 and Figure S136). Having successfully identified the living condition for ethylene polymerization with the bis-**2a**-DHFC complex, we subsequently exploredtriblock formation. Using the bis-**2a**-DHFC complex, ethylene polymerization was performed for 2 h, and MA monomer was added to the reaction mixture while the temperature was kept low (section 8.2 in the Supporting Information). The reaction was used for block copolymerization and analysis of the generated macro-chelate. ^{1}H NMR analysis of the macrochelate shows a 1:2 ratio of the ester linkage to the diimine ligand, which indicates the insertion of MA into Pd-PE chains on both sides (Figure S138). Free radical polymerization of MA under blue light with the addition of an ancillary ligand was performed, affording triblock copolymers (Figure 18). The product obtained after the light reaction was purified by the centrifugation method to
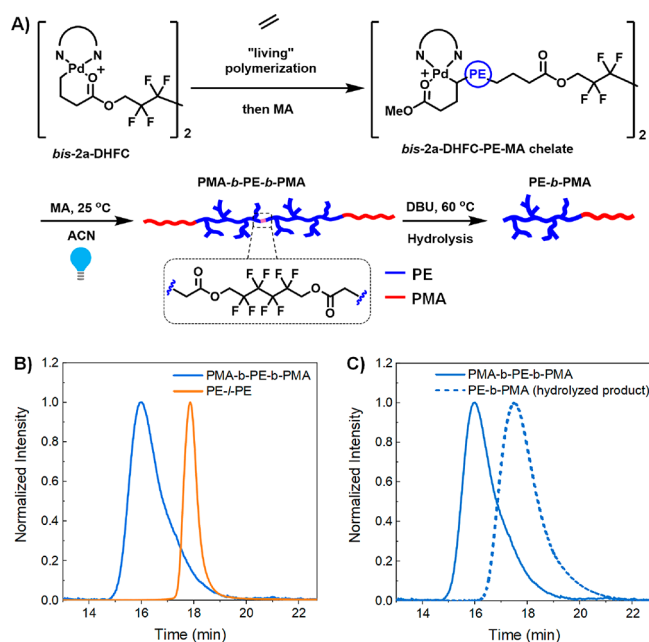

Figure 18. (A) Synthesis of PMA-*b*-PE-*b*-PMA triblock copolymers (Table 1, entry 11) and hydrolysis experiment, GPC traces of (B) the triblocks after the light reaction and their PE precursor and (C) before and after hydrolysis.

remove unreacted PE and exhibited a mono distribution over triple-detection SEC/GPC analysis (Table 1, entry 11, and Figure S139). The identity of the PMA-*b*-PE-*b*-PMA triblocks was also evidenced through a cleavage experiment with DBU, yielding a single trace for the resultant PE-*b*-PMA diblock copolymers. It is noticeable that the molar ratio of ethylene and MA repeating units remained unchanged before and after the hydrolysis, which also points toward the uniform activity of both palladium centers (Figure S140). Further GPC and NMR data can be found in section 8.2 in the Supporting Information. DSC, SAXS, and DLS data again confirm the block structure of the materials (Figure S141).

■ CONCLUSION

The development of next-generation materials will arise from orthogonal platforms that can seamlessly generate polyolefin−polar block copolymers, which stem from approaches that seek to combine multiple polymerization techniques into a single platform. Herein, we report a mechanism in which coordination insertion and radical polymerization techniques are bridged through the use of cationic diimine Pd(II) complexes. The experimental results illustrate the interplay among chain walking, chelation, and radical initiation for block copolymer synthesis. Because chelates derived from methyl acrylate insertion serve as a thermodynamic sink in copolymerization with olefins, stable macroinitiators can be prepared with tunable molecular weights in a facile manner. The photochemically inactive chelate requires reversible opening while also avoiding chain transfer, and it is this subtle interplay that has been overlooked and has prevented comparable systems from achieving block copolymers in a similar manner. The mechanism of radical generation is now understood to follow a series of steps in which opening of the chelate is facilitated by a coordinating ligand first, and subsequent chain walking allows access to the carbon α to the carbonyl moiety. This bond is suitable for homolysis in

blue light and generates a polyolefin macroradical capable of free radical polymerization of methyl acrylate, ethyl acrylate, and methyl methacrylate. Radical trapping studies combined with NMR, EPR, and MS have identified these intermediates within the mechanism and have led to improvements in the synthesis. Access to a broad range in molecular weights and compositions for block copolymers has been demonstrated. We have shown for the first time that this mechanism is suitable for a one-pot synthesis of polyethylene-*b*-polyacrylate block copolymers. Additionally, a binuclear palladium(II) catalyst has been synthesized with living olefin polymerization kinetics, and subsequent BAB triblock copolymers have been prepared in a similar one-pot fashion with acrylate-olefin-acrylate structures. With the expansion of the scope and identification of key requirements for a successful reaction, a new perspective toward triggering homolysis in chain-walking catalysts with external stimuli can finally bridge the gap in metal−organic catalysts to access amphiphilic block copolymers.

■ ABBREVIATIONS

Abbreviations of related structures can be found in section 2 of the Supporting Information.

■ ASSOCIATED CONTENT

ⓈⒾ Supporting Information

The Supporting Information is available free of charge at https://pubs.acs.org/doi/10.1021/jacs.0c10588.

> Experimental procedures, characterization of key intermediates, and additional spectroscopic data (PDF)
>
> Details of the crystal structure data and refinements (PDF)
>
> Crystallographic data (CIF)
>
> Crystallographic data (CIF)
>
> Crystallographic data (CIF)

■ AUTHOR INFORMATION

Corresponding Authors

Dain B. Beezer − *Department of Chemistry, Center of Excellence in Polymer Chemistry (CEPC), University of Houston, Houston, Texas 77004, United States;* Email: dbeezer@fisk.edu

Eva Harth − *Department of Chemistry, Center of Excellence in Polymer Chemistry (CEPC), University of Houston, Houston, Texas 77004, United States;* orcid.org/0000-0001-5553-0365; Email: harth@uh.edu

Authors

Huong Dau − *Department of Chemistry, Center of Excellence in Polymer Chemistry (CEPC), University of Houston, Houston, Texas 77004, United States*

Anthony Keyes − *Department of Chemistry, Center of Excellence in Polymer Chemistry (CEPC), University of Houston, Houston, Texas 77004, United States*

Hatice E. Basbug Alhan − *Department of Chemistry, Center of Excellence in Polymer Chemistry (CEPC), University of Houston, Houston, Texas 77004, United States*

Estela Ordonez − *Department of Chemistry, Center of Excellence in Polymer Chemistry (CEPC), University of Houston, Houston, Texas 77004, United States*

Enkhjargal Tsogtgerel − *Department of Chemistry, Center of Excellence in Polymer Chemistry (CEPC), University of Houston, Houston, Texas 77004, United States*

Anthony P. Gies − *The Dow Chemical Company, Lake Jackson, Texas 77566, United States;* orcid.org/0000-0002-3558-593X

Evelyn Auyeung − *The Dow Chemical Company, Lake Jackson, Texas 77566, United States*

Zhe Zhou − *The Dow Chemical Company, Lake Jackson, Texas 77566, United States;* orcid.org/0000-0003-0869-2112

Asim Maity − *Department of Chemistry, Texas A&M University, College Station, Texas 77843, United States;* orcid.org/0000-0002-5923-8596

Anuvab Das − *Department of Chemistry, Texas A&M University, College Station, Texas 77843, United States;* orcid.org/0000-0002-9344-4414

David C. Powers − *Department of Chemistry, Texas A&M University, College Station, Texas 77843, United States*

Complete contact information is available at:
https://pubs.acs.org/10.1021/jacs.0c10588

■ ACKNOWLEDGMENTS

■ REFERENCES

(1) Boffa, L. S.; Novak, B. M. Copolymerization of Polar Monomers with Olefins Using Transition-Metal Complexes. *Chem. Rev.* **2000**, *100* (4), 1479−1494.

(2) (a) Mayes, A. M.; Olvera de la Cruz, M. Cylindrical versus spherical micelle formation in block copolymer/homopolymer blends. *Macromolecules* **1988**, *21* (8), 2543−2547. (b) Lyatskaya, Y.; Gersappe, D.; Gross, N. A.; Balazs, A. C. Designing Compatibilizers To Reduce Interfacial Tension in Polymer Blends. *J. Phys. Chem.* **1996**, *100* (5), 1449−1458. (c) Janert, P. K.; Schick, M. Phase Behavior of Binary Homopolymer/Diblock Blends: Temperature and Chain Length Dependence. *Macromolecules* **1998**, *31* (4), 1109−1113. (d) Rebizant, V.; Venet, A.-S.; Tournilhac, F.; Girard-Reydet, E.; Navarro, C.; Pascault, J.-P.; Leibler, L. Chemistry and Mechanical Properties of Epoxy-Based Thermosets Reinforced by Reactive and

Nonreactive SBMX Block Copolymers. *Macromolecules* **2004**, *37* (21), 8017−8027. (e) Ruokolainen, J.; Mezzenga, R.; Fredrickson, G. H.; Kramer, E. J.; Hustad, P. D.; Coates, G. W. Morphology and Thermodynamic Behavior of Syndiotactic Polypropylene-Poly-(ethylene-co-propylene) Block Polymers Prepared by Living Olefin Polymerization. *Macromolecules* **2005**, *38* (3), 851−860. (f) Robinson, J. W.; Zhou, Y.; Qu, J.; Bays, J. T.; Cosimbescu, L. Highly branched polyethylenes as lubricant viscosity and friction modifiers. *React. Funct. Polym.* **2016**, *109*, 52−55. (g) Wang, F.; Lei, S.; Li, C.; Ou, J.; Xue, M.; Li, W. Superhydrophobic Cu Mesh Combined with a Superoleophilic Polyurethane Sponge for Oil Spill Adsorption and Collection. *Ind. Eng. Chem. Res.* **2014**, *53* (17), 7141−7148.

(3) (a) Ruzette, A. V.; Leibler, L. Block copolymers in tomorrow's plastics. *Nat. Mater.* **2005**, *4* (1), 19−31. (b) Leone, A. K.; Dewyer, A. L.; Kubo, T.; Zimmerman, P. M.; McNeil, A. J. Toward one-pot olefin/thiophene block copolymers using an in situ ligand exchange. *J. Polym. Sci., Part A: Polym. Chem.* **2019**, *57* (14), 1601−1605. (c) Souther, K. D.; Leone, A. K.; Vitek, A. K.; Palermo, E. F.; LaPointe, A. M.; Coates, G. W.; Zimmerman, P. M.; McNeil, A. J. Trials and tribulations of designing multitasking catalysts for olefin/thiophene block copolymerizations. *J. Polym. Sci., Part A: Polym. Chem.* **2018**, *56* (1), 132−137.

(4) (a) Dommanget, C.; D'Agosto, F.; Monteil, V. Polymerization of Ethylene through Reversible Addition-Fragmentation Chain Transfer (RAFT). *Angew. Chem., Int. Ed.* **2014**, *53* (26), 6683−6686. (b) Wolpers, A.; Bergerbit, C.; Ebeling, B.; D'Agosto, F.; Monteil, V. Aromatic Xanthates and Dithiocarbamates for the Polymerization of Ethylene through Reversible Addition-Fragmentation Chain Transfer (RAFT). *Angew. Chem., Int. Ed.* **2019**, *58* (40), 14295−14302. (c) Dai, S.; Chen, C. Palladium-Catalyzed Direct Synthesis of Various Branched, Carboxylic Acid-Functionalized Polyolefins: Characterization, Derivatization, and Properties. *Macromolecules* **2018**, *51* (17), 6818−6824. (d) Chen, M.; Yang, B.; Chen, C. Redox-Controlled Olefin (Co)Polymerization Catalyzed by Ferrocene-Bridged Phosphine-Sulfonate Palladium Complexes. *Angew. Chem., Int. Ed.* **2015**, *54* (51), 15520−15524. (e) Carrow, B. P.; Nozaki, K. Synthesis of Functional Polyolefins Using Cationic Bisphosphine Monoxide-Palladium Complexes. *J. Am. Chem. Soc.* **2012**, *134* (21), 8802−8805. (f) Chai, Y.; Wang, L.; Liu, D.; Wang, Z.; Run, M.; Cui, D. Polar-Group Activated Isospecific Coordination Polymerization of ortho-Methoxystyrene: Effects of Central Metals and Ligands. *Chem. - Eur. J.* **2019**, *25* (8), 2043−2050.

(5) Keyes, A.; Basbug Alhan, H. E.; Ordonez, E.; Ha, U.; Beezer, D. B.; Dau, H.; Liu, Y.-S.; Tsogtgerel, E.; Jones, G. R.; Harth, E. Olefins and Vinyl Polar Monomers: Bridging the Gap for Next Generation Materials. *Angew. Chem., Int. Ed.* **2019**, *58* (36), 12370−12391.

(6) (a) Tempel, D. J.; Johnson, L. K.; Huff, R. L.; White, P. S.; Brookhart, M. Mechanistic Studies of Pd(II)-α-Diimine-Catalyzed Olefin Polymerizations1. *J. Am. Chem. Soc.* **2000**, *122* (28), 6686−6700. (b) O'Connor, K. S.; Lamb, J. R.; Vaidya, T.; Keresztes, I.; Klimovica, K.; LaPointe, A. M.; Daugulis, O.; Coates, G. W. Understanding the Insertion Pathways and Chain Walking Mechanisms of α-Diimine Nickel Catalysts for α-Olefin Polymerization: A 13C NMR Spectroscopic Investigation. *Macromolecules* **2017**, *50* (18), 7010−7027. (c) Johnson, L. K.; Mecking, S.; Brookhart, M. Copolymerization of Ethylene and Propylene with Functionalized Vinyl Monomers by Palladium(II) Catalysts. *J. Am. Chem. Soc.* **1996**, *118* (1), 267−268. (d) Mecking, S.; Johnson, L. K.; Wang, L.; Brookhart, M. Mechanistic Studies of the Palladium-Catalyzed Copolymerization of Ethylene and α-Olefins with Methyl Acrylate. *J. Am. Chem. Soc.* **1998**, *120* (5), 888−899.

(7) (a) Albéniz, A. C.; Espinet, P.; López-Fernández, R. Polymerization of Acrylates by Neutral Palladium Complexes. Isolation of Complexes at the Initial Steps. *Organometallics* **2003**, *22* (21), 4206−4212. (b) López-Fernández, R.; Carrera, N.; Albéniz, A. C.; Espinet, P. Dual Behavior of Cationic Palladium Pentafluorophenyl Complexes as Catalysts for the Homopolymerization of Acrylates and of Nonpolar Olefins. *Organometallics* **2009**, *28* (17), 4996−5001. (c) Chen, Y.; Mandal, S.; Sen, A. Synthesis of (N-O)-Ligated

Palladium(II) Complexes and Their Use in Ethene Homopolymerization and Norbornene Copolymerizations. *Organometallics* **2010**, *29* (14), 3160−3168. (d) Keyes, A.; Basbug Alhan, H. E.; Ha, U.; Liu, Y.-S.; Smith, S. K.; Teets, T. S.; Beezer, D. B.; Harth, E. Light as a Catalytic Switch for Block Copolymer Architectures: Metal-Organic Insertion/Light Initiated Radical (MILRad) Polymerization. *Macromolecules* **2018**, *51* (18), 7224−7232. (e) Keyes, A.; Dau, H.; Basbug Alhan, H. E.; Ha, U.; Ordonez, E.; Jones, G. R.; Liu, Y.-S.; Tsogtgerel, E.; Loftin, B.; Wen, Z.; Wu, J. I.; Beezer, D. B.; Harth, E. Metal-organic insertion light initiated radical (MILRad) polymerization: photo-initiated radical polymerization of vinyl polar monomers with various palladium diimine catalysts. *Polym. Chem.* **2019**, *10* (23), 3040−3047. (f) Xiang, P.; Ye, Z. Homo- and Co-polymerization of norbornene and methyl acrylate with Pd-diimine catalysts. *J. Organomet. Chem.* **2015**, *798*, 429−436.

(8) (a) Leblanc, A.; Grau, E.; Broyer, J.-P.; Boisson, C.; Spitz, R.; Monteil, V. Homo- and Copolymerizations of (Meth)Acrylates with Olefins (Styrene, Ethylene) Using Neutral Nickel Complexes: A Dual Radical/Catalytic Pathway. *Macromolecules* **2011**, *44* (9), 3293−3301. (b) Ölscher, F.; Göttker-Schnetmann, I.; Monteil, V.; Mecking, S. Role of Radical Species in Salicylaldiminato Ni(II) Mediated Polymer Chain Growth: A Case Study for the Migratory Insertion Polymerization of Ethylene in the Presence of Methyl Methacrylate. *J. Am. Chem. Soc.* **2015**, *137* (46), 14819−14828.

(9) Gottfried, A. C.; Brookhart, M. Living and Block Copolymerization of Ethylene and α-Olefins Using Palladium(II)-α-Diimine Catalysts. *Macromolecules* **2003**, *36* (9), 3085−3100.

(10) Gottfried, A. C.; Brookhart, M. Living Polymerization of Ethylene Using Pd(II) α-Diimine Catalysts. *Macromolecules* **2001**, *34* (5), 1140−1142.

(11) Haven, J. J.; Junkers, T. Online Monitoring of Polymerizations: Current Status. *Eur. J. Org. Chem.* **2017**, *2017* (44), 6474−6482.

(12) Dall'Anese, A.; Rosar, V.; Cusin, L.; Montini, T.; Balducci, G.; D'Auria, I.; Pellecchia, C.; Fornasiero, P.; Felluga, F.; Milani, B. Palladium-Catalyzed Ethylene/Methyl Acrylate Copolymerization: Moving from the Acenaphthene to the Phenanthrene Skeleton of α-Diimine Ligands. *Organometallics* **2019**, *38* (19), 3498−3511.

(13) (a) Boisvert, L.; Denney, M. C.; Hanson, S. K.; Goldberg, K. I. Insertion of Molecular Oxygen into a Palladium(II) Methyl Bond: A Radical Chain Mechanism Involving Palladium(III) Intermediates. *J. Am. Chem. Soc.* **2009**, *131* (43), 15802−15814. (b) Smoll, K. A.; Kaminsky, W.; Goldberg, K. I. Photolysis of Pincer-Ligated PdII-Me Complexes in the Presence of Molecular Oxygen. *Organometallics* **2017**, *36* (7), 1213−1216.

(14) Nagel, M.; Sen, A. Intermediacy of Radicals in Rearrangement and Decomposition of Metal-Alkyl Species: Relevance to Metal-Mediated Polymerization of Polar Vinyl Monomers. *Organometallics* **2006**, *25* (20), 4722−4724.

(15) Philipp, D. M.; Muller, R. P.; Goddard, W. A.; Storer, J.; McAdon, M.; Mullins, M. Computational Insights on the Challenges for Polymerizing Polar Monomers. *J. Am. Chem. Soc.* **2002**, *124* (34), 10198−10210.

(16) Borkar, S.; Yennawar, H.; Sen, A. Methacrylate Insertion into Cationic Diimine Palladium(II)-Alkyl Complexes and the Synthesis of Poly(alkene-block-alkene/carbon monoxide) Copolymers. *Organometallics* **2007**, *26* (19), 4711−4714.

(17) Dikanov, S. A.; Crofts, A. R., Electron Paramegnetic Resonance Spectroscopy. In *Handbook of Applied Solid State Spectroscopy*; Vij, D. R., Ed.; Springer US: Boston, MA, 2006; pp 97−149.

(18) (a) Ratushnyy, M.; Kvasovs, N.; Sarkar, S.; Gevorgyan, V. Visible-Light-Induced Palladium-Catalyzed Generation of Aryl Radicals from Aryl Triflates. *Angew. Chem., Int. Ed.* **2020**, *59* (26), 10316−10320. (b) Huang, H.-M.; Koy, M.; Serrano, E.; Pflüger, P. M.; Schwarz, J. L.; Glorius, F. Catalytic radical generation of π-allylpalladium complexes. *Nat. Catal.* **2020**, *3* (4), 393−400.

(19) (a) Chen, Y.; Hu, Z.; Xu, D.; Yu, Y.; Tang, X.; Guo, H. Studies of Free Radical Polymerization Initiated by Visible Light Photoredox Catalysis. *Macromol. Chem. Phys.* **2015**, *216* (10), 1055−1060. (b) Su, W.-F., Radical Chain Polymerization. In *Principles of Polymer Design*

and Synthesis; Springer Berlin Heidelberg: Berlin, Heidelberg, 2013; pp 137−183.

(20) Nakamura, Y.; Lee, R.; Coote, M. L.; Yamago, S. Termination Mechanism of the Radical Polymerization of Acrylates. *Macromol. Rapid Commun.* **2016**, *37* (6), 506−513.

(21) Chen, Z.; Brookhart, M. Exploring Ethylene/Polar Vinyl Monomer Copolymerizations Using Ni and Pd α-Diimine Catalysts. *Acc. Chem. Res.* **2018**, *51* (8), 1831−1839.

(22) Kermagoret, A.; Debuigne, A.; Jérôme, C.; Detrembleur, C. Precision design of ethylene- and polar-monomer-based copolymers by organometallic-mediated radical polymerization. *Nat. Chem.* **2014**, *6* (3), 179−187.

(23) Shultz, L. H.; Tempel, D. J.; Brookhart, M. Palladium(II) β-Agostic Alkyl Cations and Alkyl Ethylene Complexes: Investigation of Polymer Chain Isomerization Mechanisms. *J. Am. Chem. Soc.* **2001**, *123* (47), 11539−11555.

(24) Meira, G. R.; Silveston, P. L. Polymerization Under Modulation. In *Periodic Operation of Chemical Reactors*; Silveston, P. L., Hudgins, R. R., Eds.; Butterworth-Heinemann: Oxford, 2013; Chapter 7, pp 171−203.

(25) Wilczek-Vera, G.; Yu, Y.; Waddell, K.; Danis, P. O.; Eisenberg, A. Detailed structural analysis of diblock copolymers by matrix-assisted laser desorption/ionization time-of-flight mass spectrometry. *Rapid Commun. Mass Spectrom.* **1999**, *13* (9), 764−777.

(26) Crecelius, A. C.; Becer, C. R.; Knop, K.; Schubert, U. S. Block length determination of the block copolymer mPEG-b-PS using MALDI-TOF MS/MS. *J. Polym. Sci., Part A: Polym. Chem.* **2010**, *48* (20), 4375−4384.

(27) Town, J. S.; Jones, G. R.; Haddleton, D. M. MALDI-LID-ToF/ToF analysis of statistical and diblock polyacrylate copolymers. *Polym. Chem.* **2018**, *9* (37), 4631−4641.

(28) Desurmont, G.; Tokimitsu, T.; Yasuda, H. First Controlled Block Copolymerizations of Higher 1-Olefins with Polar Monomers Using Metallocene Type Single Component Lanthanide Initiators. *Macromolecules* **2000**, *33* (21), 7679−7681.

(29) Daimon, H.; Okitsu, H.; Kumanotani, J. Glass Transition Behaviors of Random and Block Copolymers and Polymer Blends of Styrene and Cyclododecyl Acrylate. I. Glass Transition Temperatures. *Polym. J.* **1975**, *7* (4), 460−466.

(30) Dai, S.; Sui, X.; Chen, C. Highly Robust Palladium(II) α-Diimine Catalysts for Slow-Chain-Walking Polymerization of Ethylene and Copolymerization with Methyl Acrylate. *Angew. Chem., Int. Ed.* **2015**, *54* (34), 9948−9953.

(31) (a) Van Horn, R. M.; Steffen, M. R.; O'Connor, D. Recent progress in block copolymer crystallization. *Polym. Cryst.* **2018**, *1* (4), No. e10039. (b) Nandan, B.; Hsu, J. Y.; Chen, H. L. Crystallization Behavior of Crystalline-Amorphous Diblock Copolymers Consisting of a Rubbery Amorphous Block. *J. Macromol. Sci., Polym. Rev.* **2006**, *46* (2), 143−172. (c) Shiomi, T.; Takeshita, H.; Kawaguchi, H.; Nagai, M.; Takenaka, K.; Miya, M. Crystallization and Structure Formation of Block Copolymers Containing a Rubbery Amorphous Component. *Macromolecules* **2002**, *35* (21), 8056−8065.

(32) (a) Yan, T.; Guironnet, D. Amphiphilic triblock copolymers containing polypropylene as the middle block. *Angew. Chem., Int. Ed.* **2020**, DOI: 10.1002/anie.202009165. (b) Makio, H.; Fujita, T. Synthesis of Chain-End Functionalized Polyolefins with a Bis-(phenoxy imine) Titanium Catalyst. *Macromol. Rapid Commun.* **2007**, *28* (6), 698−703.

(33) (a) Wang, F.; Chen, C. A continuing legend: the Brookhart-type α-diimine nickel and palladium catalysts. *Polym. Chem.* **2019**, *10* (19), 2354−2369. (b) Takano, S.; Takeuchi, D.; Osakada, K.; Akamatsu, N.; Shishido, A. Dipalladium Catalyst for Olefin Polymerization: Introduction of Acrylate Units into the Main Chain of Branched Polyethylene. *Angew. Chem., Int. Ed.* **2014**, *53* (35), 9246−9250. (c) Wang, R.; Sui, X.; Pang, W.; Chen, C. Ethylene Polymerization by Xanthene-Bridged Dinuclear α-Diimine Ni^II Complexes. *ChemCatChem* **2016**, *8* (2), 434−440. (d) Ye, J.; Ye, Z. Living" Polymerization of Ethylene and 1-Hexene Using Novel Binuclear Pd-Diimine Catalysts. *Polymers* **2017**, *9* (12), 282−303.